Journal of *Marine Science and Engineering*

MDPI

Article

Frequency-Based Analysis of Matching Accuracy Between Satellite Radio Frequency and AIS Data for Ship Identification

Chan-Su Yang [1,2,3,*] and Sree Juwel Kumar Chowdhury [1,2]

[1] Maritime Security and Safety Research Center, Korea Institute of Ocean Science & Technology, Busan 49111, Republic of Korea; jusau65@kiost.ac.kr
[2] Department of Convergence Study on the Ocean Science and Technology, Ocean Science and Technology School, National Korea Maritime & Ocean University, Busan 49111, Republic of Korea
[3] Marine Technology and Convergence Engineering, University of Science & Technology, Daejeon 34111, Republic of Korea
* Correspondence: yangcs@kiost.ac.kr

Abstract: Vessels can deactivate their Automatic Identification System (AIS) to operate undetected and potentially engage in illegal activities. To address this, satellite-based radio frequency (RF) data are increasingly being used for identifying such vessels. This study evaluates the matching accuracy among RF and AIS data based on the frequency and distance. RF data were acquired on 22 September, 25 September, and 7 December 2023. According to the frequency range, the dataset was separated into frequency-1 (3.024–3.077 GHz) and frequency-2 (9.3734–9.4249 GHz). Six distance thresholds (2 km, 3 km, 6 km, 8 km, 13 km, and 18 km) were employed for the matching process. The results depicted that the average matching rates were 95%, 92%, and 92% for the RF dataset on 22 September, 25 September, and 7 December, respectively. Additionally, the results revealed that the matching rates decreased with distance, e.g., for the RF dataset on 22 September, the average highest matching rate (47%) was found at a 2 km distance and the minimum matching rate (0.9%) was observed at an 18 km distance. Furthermore, the analysis delineated that frequency-2 consistently exceeded frequency-1, particularly at longer distances, showing a more stable trend in matching accuracy.

Keywords: radio frequency; AIS; matching rate; maritime surveillance

check for updates

Academic Editors: Nam Kyu Park, Livia Maglić, Ana Peric Hadzic, Marina Zanne and Lovro Maglić

Received: 12 December 2024
Revised: 10 January 2025
Accepted: 16 January 2025
Published: 21 January 2025

Citation: Yang, C.-S.; Chowdhury, S.J.K. Frequency-Based Analysis of Matching Accuracy Between Satellite Radio Frequency and AIS Data for Ship Identification. *J. Mar. Sci. Eng.* **2025**, *13*, 191. https://doi.org/10.3390/jmse13020191

Copyright: © 2025 by the authors. Licensee MDPI, Basel, Switzerland. This article is an open access article distributed under the terms and conditions of the Creative Commons Attribution (CC BY) license (https://creativecommons.org/licenses/by/4.0/).

1. Introduction

Maritime freight transport is a critical component of global trade, accounting for approximately 90% of international freight transport [1]. Daily, over 50,000 vessels navigate the world's oceans, facilitating the exchange of goods and resources across vast distances [2]; consequently, maritime traffic accidents happen once in a while due to this extensive scale of maritime operations [3]. Therefore, the increasing complexity and high volume of maritime activities emphasize the significant demand for advanced surveillance systems to ensure safety, enhance security, and protect the environment within global maritime domains. Among the diverse resources utilized for maritime surveillance, the Automatic Identification System (AIS) and Synthetic Aperture Radar (SAR) are recognized as the most efficient components for monitoring and analyzing vessel traffic.

The International Maritime Organization (IMO) introduced the AIS to enhance maritime surveillance and reduce collision risks [4]. Since 2004, the IMO has mandated the installation of AIS equipment on all international vessels with a gross tonnage of 300 or more and on all passenger ships, ensuring improved vessel tracking and safety [5]. The AIS

is specifically designed to enhance maritime safety by enabling the exchange of real-time vessel movement data, allowing for the monitoring and analysis of navigational intentions to reduce collision risks [6]. Each vessel equipped with the AIS automatically broadcasts key information, including its Maritime Mobile Service Identity (MMSI), latitude, longitude, course, heading, and speed [7]. These data are transmitted in real-time, employing very high-frequency radio waves, to onshore AIS receiving stations [8]. The real-time transmission of positional data allows neighboring vessels to detect and avoid potential collisions, enhancing safety at sea. Additionally, the information received by onshore vessel traffic services stations plays a crucial role in effective traffic management and navigation guidance, ensuring smooth maritime operations. Additionally, to broaden the coverage of maritime monitoring, low Earth orbit satellites have been specifically designed to receive AIS messages, a system referred to as a satellite-based AIS (S-AIS) [8]. These satellites use standard terrestrial AIS receivers to retrieve signals across extended coastal regions [8]. By overcoming the limitations of ground-based AIS systems, S-AIS provides global coverage, addressing gaps in ocean surveillance and ensuring continuous monitoring in remote and expansive maritime areas [9]. Consequently, the prompt increase in the spatial and temporal volume of AIS data has significantly contributed to its extensive application in maritime research and operations, including the analysis of traffic patterns, ship behavior, anomaly detection, and continuous vessel monitoring [3,10,11]. In addition, the key areas of study leveraging AIS data include ship trajectory prediction [12], collision risk assessment [13], and classification of ship types based on AIS-derived trajectories [14]. In addition to AIS data, SAR data are increasingly utilized for maritime surveillance due to their high-resolution imaging capabilities, which operate effectively under all weather conditions and at any time of day or night [15]. Numerous studies have leveraged SAR data for ship detection by employing window-based target detection methods and advanced deep learning techniques, such as region-based convolutional neural networks (CNNs), single shot multi-box detector (SSD), and You Only Look Once (YOLO) algorithms [16–18]. To assess the detection results, AIS data are utilized as a complementary source, providing additional positional information [15]. However, vessels may deactivate their AIS, becoming 'dark vessels', which could indicate potential involvement in illegal activities. In addition, AIS spoofing, which involves the deliberate manipulation or falsification of vessel tracking information, is often used to mislead the vessel monitoring systems and maritime crews, e.g., by generating ghost ships or broadcasting false emergency messages [19]. These spoofing can conceal the identities and operations of vessels involved in illicit activities such as illegal, unreported, and unregulated (IUU) fishing, identity laundering, smuggling, and evasion of international sanctions. To track such vessels, satellite-based radio frequency (RF) data are being increasingly utilized [20].

RF data refers to the measurement of electromagnetic radiation across a broad frequency spectrum, ranging from 300 GHz to 9 kHz [21]. These frequencies are emitted when radio waves oscillate within the electromagnetic spectrum. RF detection systems are used to capture and geolocate these emissions, which specifically target RF signals emitted by maritime vessels. These signals are often associated with navigation radar systems essential for safe navigation and collision avoidance [22]. Although AIS data can be susceptible to manipulation, RF-based monitoring provides a more dependable approach for tracking vessel activity at sea, regardless of weather conditions, time of day, or other environmental factors. RF data plays a crucial role in detecting and localizing non-cooperative vessels by capturing intercepted communication signals and radar emissions, thereby addressing significant limitations posed by other systems. Numerous studies have been conducted to identify and monitor 'dark vessels'—ships operating without valid AIS data—by leading companies specializing in space-based RF services. A case study conducted by Unseenlabs

using RF data involved monitoring a fishing fleet in the northern Arabian Sea, and the study results displayed that approximately 65% of vessels were identified that had both RF and AIS signals, and, on the contrary, 35% of vessels in that region were navigating without an AIS signal, implying that these vessels were operating in dark mode [20]. Another study performed by HawkEye 360 investigated a cargo vessel that departed from Turkey and ceased transmitting AIS data for seven days, prompting concerns about its activities. Through RF signal data, HawkEye 360 was able to detect the vessel's stay at Tartus Port in Syria during the AIS termination, offering valuable insights into the vessel's movements. This case highlights the importance of RF data in tracking vessels and addressing gaps in AIS coverage, ultimately strengthening maritime monitoring and security [20]. Furthermore, ref. [23] proposed a matching approach for vessel identification by integrating RF and AIS data in the Yellow Sea region.

Although the assimilation of RF and AIS data for vessel monitoring has gained significant consideration, there has been a lack of studies assessing the matching accuracy based on frequency and distance. Therefore, this study focuses on evaluating the accuracy of matching RF and AIS data, with particular emphasis on the effects of frequency and distance. The findings of this analysis will contribute to comprehending the accuracy trends and enhance the effectiveness of maritime surveillance systems.

2. Materials and Methods

2.1. Study Area

The region encompassing the Yellow Sea and the western part of the Korea Strait is selected as the study area, which spans from 119° E to 130° E and 30° N to 38° N (Figure 1). This region is a vital economic corridor connecting Korea with other Asian nations and serves as a key hub in the Asia-Pacific logistics network. As a result, major international maritime routes are adjacent to the study area, and it acts as a significant navigating route for numerous vessels operating between Korea and other countries.

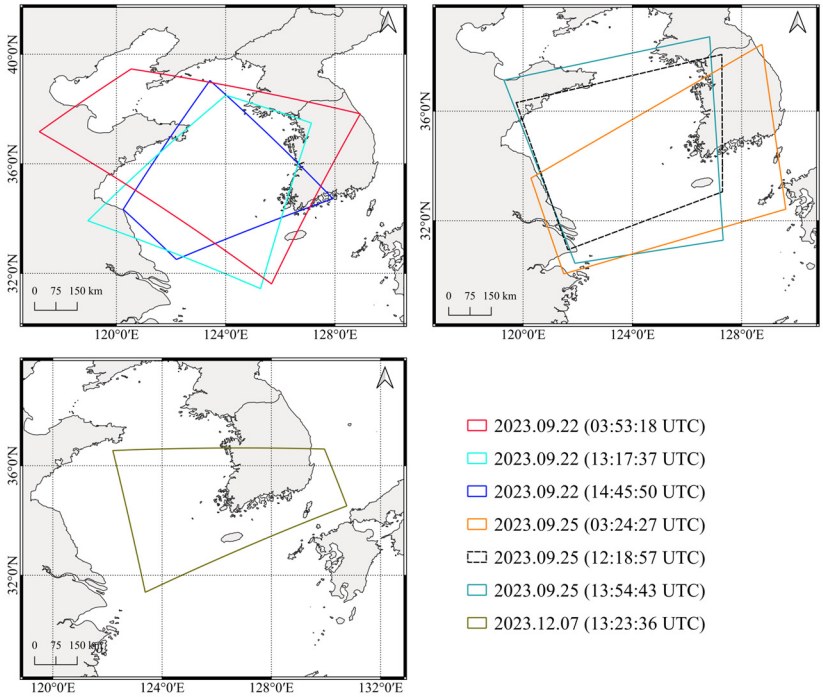


Figure 1. Location of the study area with the coverage of radio frequency data on 22 September, 25 September, and 7 December 2023.

2.2. Data

RF satellites are equipped with advanced receiving antennas that are capable of detecting signals across extensive areas. These satellites utilize advanced RF sensors to identify distinct emitters and precisely geolocate them through triangulating signals from multiple orbital perspectives [22]. In the case of maritime applications, by assigning distinct RF signals to ships at sea, this technology facilitates real-time monitoring of vessel location [22]. For this study, RF data from Unseenlabs were collected on 22 September, 25 September, and 7 December 2023. (Table 1). With a constellation of seven satellites, Unseenlabs achieves a revisit interval of approximately six hours for any given area, providing geolocation accuracy within one nautical mile [21]. The information obtained from the RF data comprised vessel ID, transmission frequency, geographic coordinates (latitude and longitude), data reliability, and accuracy. This information was obtained through signal analysis, with the frequency spectrum ranging from 3.024 GHz to 9.4249 GHz, enabling precise monitoring and identification of vessels. Furthermore, the AIS data (https://spire.com/maritime/ (accessed on 10 March 2024)) collected on 22 September, 25 September, and 7 December were used in this study, which covers the Yellow Sea and the western part of the Korea Strait. The data were acquired within a three-hour timeframe prior to and after the timestamps of the RF dataset, which enabled a comprehensive analysis of vessel movements and locations in conjunction with the RF data.

Table 1. Properties of RF data used in this study.

Date	Dataset	Time (UTC)	Frequency Range
22 September 2023	S22-RF1	03:53:17	3.0371–3.0770 GHz
		03:53:19	9.3734–9408.4 GHz
	S22-RF2	13:17:36	3.0250–3076.8 GHz
		13:17:53	9.3776–9.4217 GHz
	S22-RF3	14:44:49	3.0248–3.0768 GHz
		14:44:51	9.3769–9.4239 GHz
25 September 2023	S25-RF1	03:24:26	3.0367–3.0761 GHz
		03:24:28	9.3757–9.4233 GHz
	S25-RF2	12:18:56	3.0240–3.0765 GHz
		12:18:58	9.3784–9.4248 GHz
	S25-RF3	13:54:42	9.3742–9.4209 GHz
		13:54:44	3.0335–3.0770 GHz
7 December 2023	D07-RF	13:23:35	3.0339–3.0503 GHz
		13:23:36	9.3928–9.4249 GHz

2.3. Methodology

The overall workflow for the frequency-based analysis of matching accuracy between RF and AIS data in this study is illustrated in Figure 2. Marine radars on ships typically consist of two types: S-band (approx. 3 GHz) for long-range detection and large target tracking like ships, and X-band (approx. 9 GHz) for high-resolution imaging of smaller targets like fishing vessels [24]. To leverage their complementary strengths, most vessels are equipped with both radar types, ensuring a comprehensive understanding of the surrounding environment. Thus, the RF data were separated and categorized based on their frequency range, denoted as frequency-1 (3.024~3.077 GHz) and frequency-2 (9.3734~9.4249 GHz). Furthermore, to enhance the temporal alignment of AIS data with the RF data and address gaps in

the vessel trajectory, AIS data were interpolated at 30 min intervals. Linear interpolation was employed to estimate intermediate positions between reported AIS points, thereby ensuring a more continuous and consistent trajectory; additionally, dead reckoning (DR) positions were calculated. Subsequently, to facilitate the matching process between RF and AIS data, a series of progressively increasing distance thresholds were used, which describe the maximum acceptable distance for a logical match between the RF and AIS positions, and the distances used in this study were 2 km, 3 km, 6 km, 8 km, 13 km, and 18 km. For each RF data point, the matching process is initiated by identifying AIS positions that fall within the defined distance thresholds. The distance between each RF data point and both the original and interpolated AIS positions was calculated by using the haversine distance equation to quantify their spatial proximity. After identifying the matching positions within the specified distance, the result was defined through a flag that depicts the specific matching distance (Figure 2).

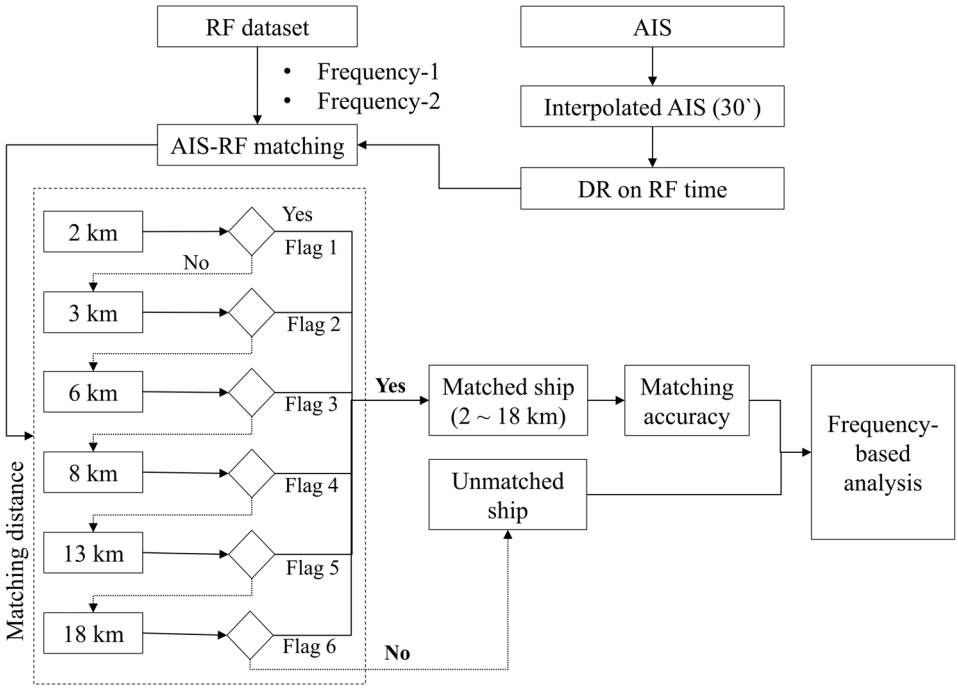


Figure 2. Schematic diagram of ship matching process using RF and AIS data. Frequency-1 and frequency-2 represent the RF data with frequency ranges from 3.024 to 3.077 GHz and 9.3734 to 9.4249 GHz, respectively.

The following flag information was used: flag 1 for the matching distance of 2 km, flag 2 for the distance of 3 km, flag 3 for the distance of 6 km, flag 4 for the distance of 8 km, flag 5 for the distance of 13 km, and flag 6 for the distance of 18 km. For each distance threshold, the matching process recorded cases where the RF-AIS distance was within the specified limit, noting the matching rate for both frequency-1 and frequency-2 separately. This step ensured that only those RF data points with corresponding AIS data within the predefined proximity were retained for further analysis. To prevent the occurrence of duplicate matches (Figure 3), vessel IDs that were successfully matched at each specified distance were systematically excluded from subsequent matching iterations at larger distances. Finally, an evaluation of matching accuracy was performed at each specified matching distance, with the results analyzed according to distinct frequency ranges. Additionally, the overall matching results for the RF dataset were calculated by averaging the matching percentage obtained at each distance.

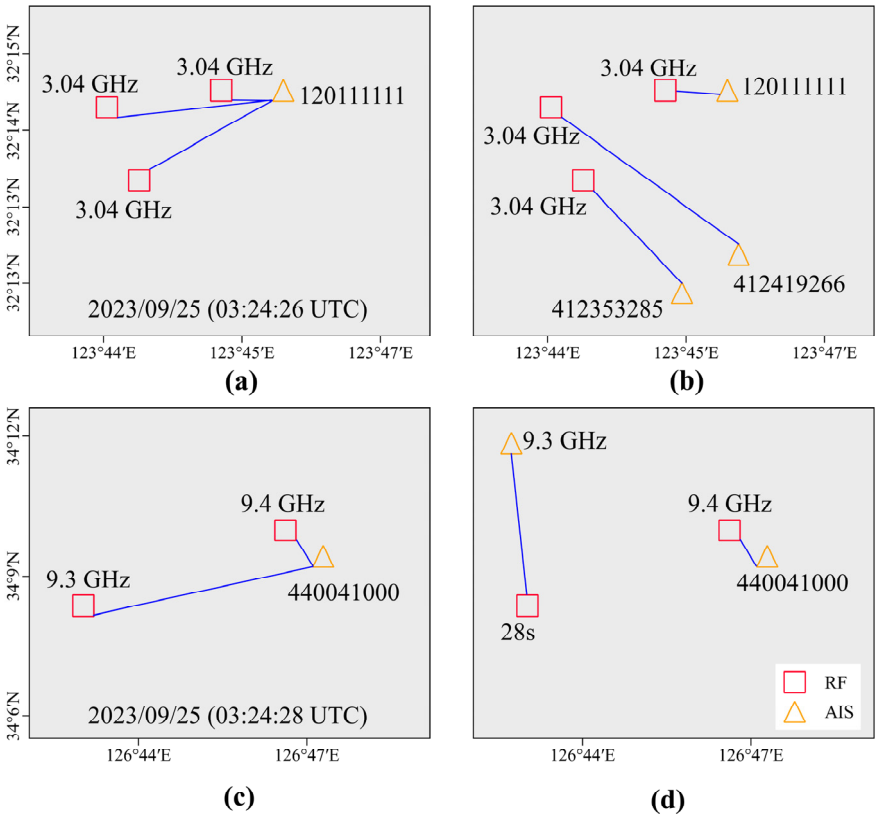


Figure 3. Example of duplicate ship matching and individual ship matching results from RF and AIS data at distinct frequencies. (**a**,**c**) Matching results from Unseenlabs and (**b**,**d**) matching results from this study. The red rectangle indicates the RF (frequency), and the amber triangle represents the AIS (Vessel ID). The blue line indicates the matching between the RF and AIS data.

3. Results

3.1. Analysis of Matching Results from RF Dataset on 22 September 2023

In the S22-RF1 dataset, a total of 1103 ship records were found, among which 498 ships' data were acquired at frequency-1 (3.04~3.08 GHz), and 605 ships' data were obtained at frequency-2 (9.37~9.41 GHz). The matching analysis between the S22-RF1 and AIS data showed that 1027 ships were successfully matched (Figure 4). At frequency-1 and frequency-2, the total number of matched ships was 452 (90%) and 575 (95%), respectively (Figure 4). For frequency-1 S22-RF1 data, the matching rate of ships at distances of 2 km, 3 km, 6 km, 8 km, 13 km, and 18 km distance was 49%, 12%, 15%, 10%, 3%, and 0.8%, respectively. For frequency-2 S22-RF1 data, the matching rate at these distances was 43%, 15%, 19%, 12%, 2%, and 1%, respectively. The overall matching rate for the S22-RF1 dataset was found to be 93%. Within the specified matching distance (2~18 km), 9% of ships remained unmatched at frequency-1 and 5% of unmatched ships were found at frequency-2.

The S22-RF2 dataset comprised a total of 805 ship records, where 582 vessels' data were obtained at frequency-1 and 223 vessels' data at frequency-2. Upon conducting the matching between S22-RF2 and AIS data, 782 ships were matched successfully (Figure 5). Of these, 566 (97%) ships were matched at frequency-1 and 216 (97%) at frequency-2. The matching rates for frequency-1 S22-RF2 data across different distance thresholds were 43% at 2 km, 21% at 3 km, 20% at 6 km, 8% at 8 km, 2% at 13 km, and 0.7% at 18 km. Similarly, for frequency-2 S22-RF2 data, the matching rates at these distances were 47%, 16%, 20%, 10%, 1%, and 0.4%, respectively. The overall matching rate for the S22-RF2 dataset was calculated at 97%. Moreover, 3% of ships were found to be unmatched at both frequencies.

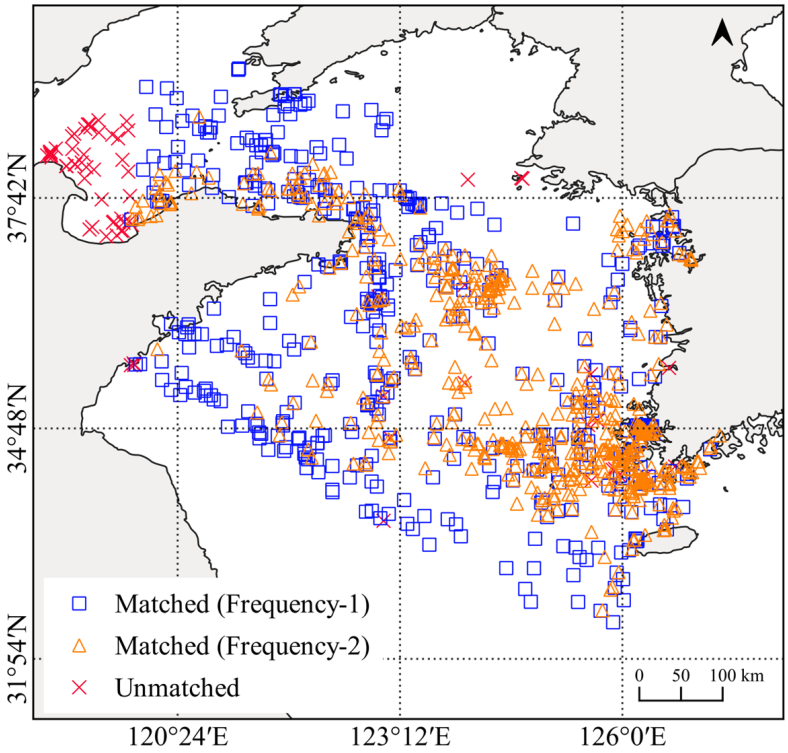


Figure 4. Identification of ships from different frequencies after matching the S22-RF1 dataset and AIS data on 22 September 2023. The blue rectangle indicates the position of the ship matched at frequency-1 (3.04~3.08 GHz), and the amber triangle represents the matched ship position at frequency-2 (9.37~9.41 GHz).

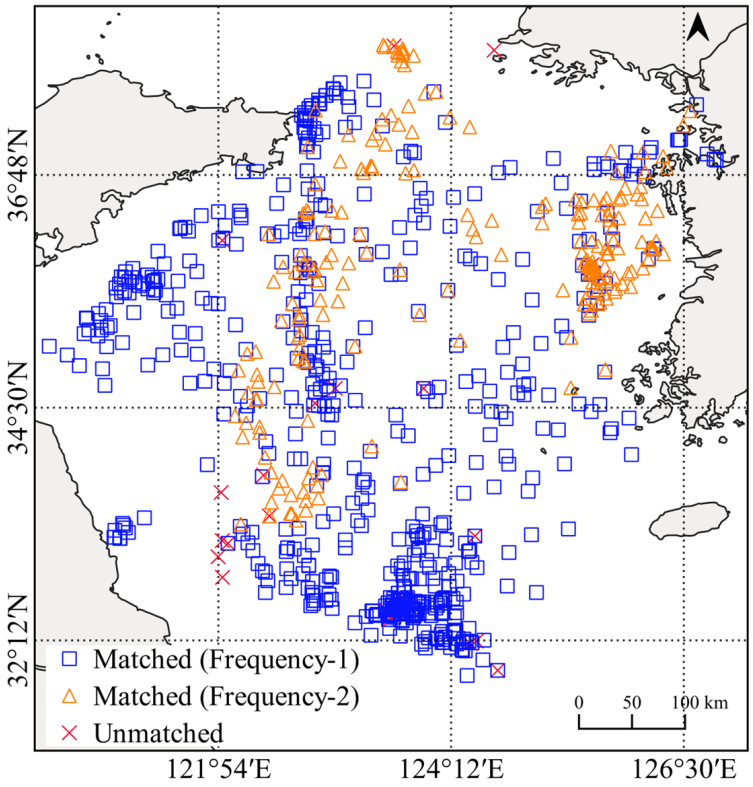


Figure 5. Ship identification results over the study area from different frequencies after matching the S22-RF2 dataset and AIS on 22 September 2023. The blue rectangle indicates the position of a matched ship at frequency-1 (3.04~3.08 GHz), and the amber triangle represents the position of a matched ship at frequency-2 (9.37~9.41 GHz).

The S22-RF3 dataset includes 778 ship records, with 428 ships' data collected at frequency-1 and 350 ships' data at frequency-2. The matching analysis between the S22-RF3 and AIS data indicated that 757 ships were successfully matched (Figure 6). Specifically, 416 ships (97%) were matched at frequency-1, while 341 ships (97%) were matched at frequency-2. The matching rates for frequency-1 S22-RF3 data across various distance thresholds were as follows: 45% at 2 km, 17% at 3 km, 25% at 6 km, 5% at 8 km, 1% at 13 km, and 0.7% at 18 km. For frequency-2 S22-RF3 data, the corresponding matching rates were 46%, 18%, 20%, 7%, 3%, and 1%, respectively. The overall matching rate for the S22-RF3 dataset was calculated to be 97%. Also, 3% of ships were determined to be unmatched at both frequencies.

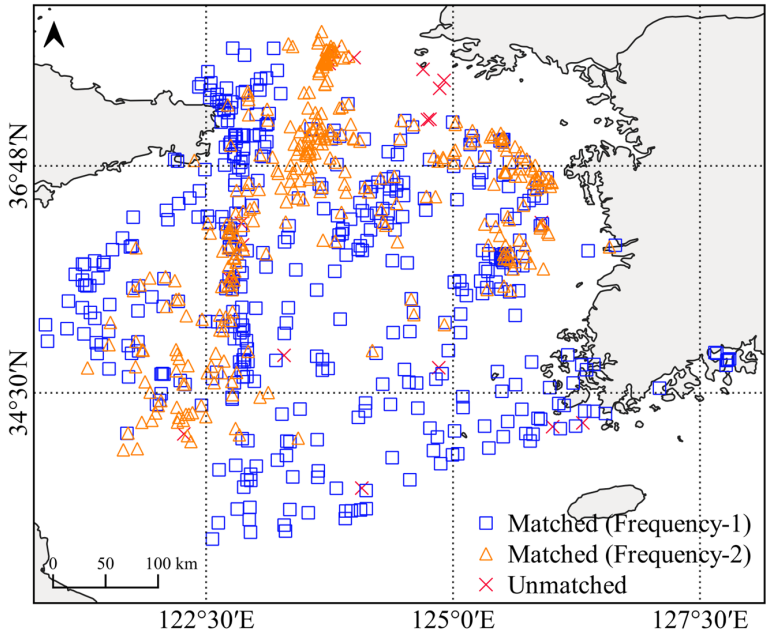


Figure 6. Ship identification results from different frequencies after matching the S22-RF3 dataset and AIS data on 22 September 2023. The blue rectangle indicates the position of a matched ship at frequency-1 (3.04~3.08 GHz), and the amber triangle represents the position of a matched ship at frequency-2 (9.37~9.41 GHz).

Table 2 displays a detailed summary of the overall analysis result for the RF dataset on 22 September 2023.

Table 2. Overview of the matching analysis for the RF dataset on 22 September 2023, detailing results for each specified distance across different frequencies.

Dataset (Frequency)	Total RF in Dataset	Total Matched Ship	Matched Ship (%)						Unmatched Ship (%)
			2 km	3 km	6 km	8 km	13 km	18 km	
S22-RF1 (Frequency-1)	498	452	49	12	15	10	3	0.8	9
S22-RF1 (Frequency-2)	605	575	43	15	19	12	2	1	5
S22-RF2 (Frequency-1)	582	566	43	21	20	8	2	0.7	3
S22-RF2 (Frequency-2)	223	216	47	16	20	10	1	0.4	3
S22-RF3 (Frequency-1)	428	416	45	17	25	5	1	0.9	3
S22-RF3 (Frequency-2)	350	341	46	18	20	7	3	1	3

3.2. Analysis of Matching Results from RF Dataset on 25 September 2023

The S25-RF1 dataset consists of 966 ship records, with 429 ships' data collected at frequency-1 and 537 ships' data at frequency-2. After performing the matching analysis between the S25-RF1 and AIS datasets, 860 ships were successfully identified (Figure 7). Within these, 376 ships (87%) were matched at frequency-1 and 484 ships (90%) at frequency-2. The matching rates for frequency-1 S25-RF1 data at different distance thresholds were 42% at 2 km, 13% at 3 km, 20% at 6 km, 7% at 8 km, 2% at 13 km, and 1% at 18 km. For frequency-2 S25-RF1 data, at the corresponding distance, the matching rates were 42%, 16%, 20%, 7%, 2%, and 1%, respectively. The overall matching accuracy for the S25-RF1 dataset was calculated to be 88%. Moreover, it was found that 13% of ships were unmatched at frequency-1, while 10% were unmatched at frequency-2.

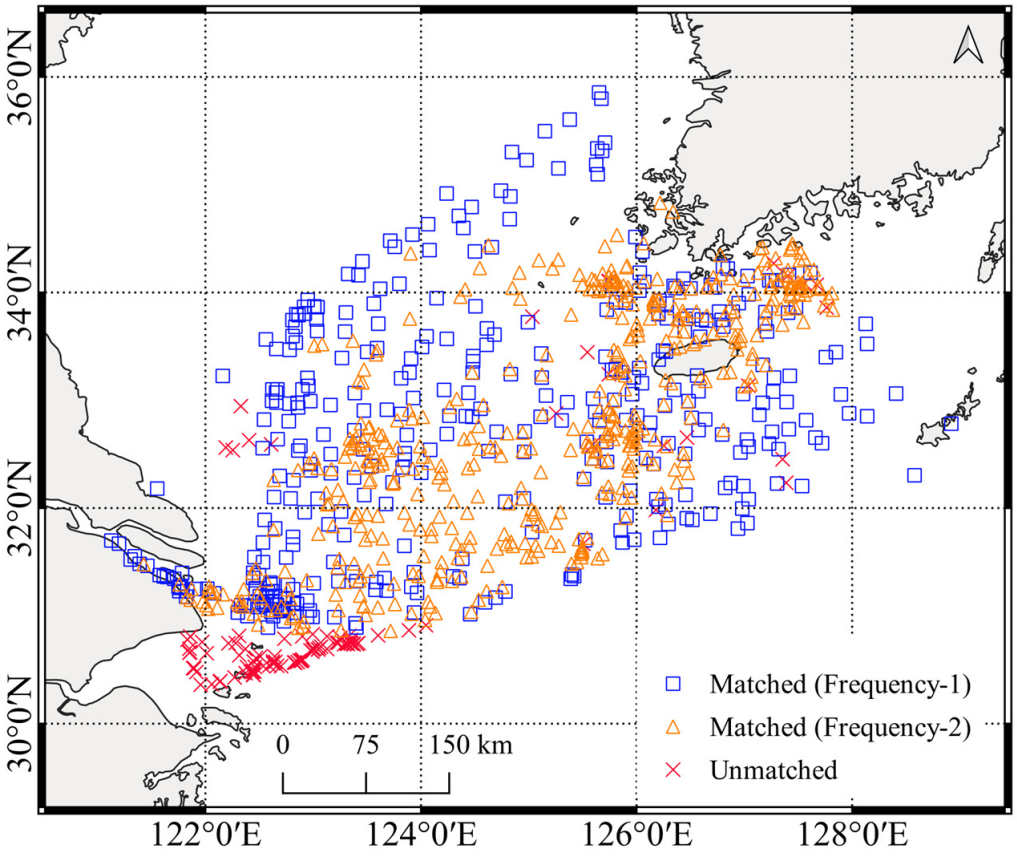


Figure 7. Identification of ships from different frequencies after matching between the S25-RF1 dataset and AIS data on 25 September 2023. The blue rectangle indicates the position of a matched ship at frequency-1 (3.04~3.08 GHz), and the amber triangle represents the position of a matched ship at frequency-2 (9.37~9.41 GHz).

A total of 922 ship records were found in the S25-RF2 dataset, among which 469 ships' data were acquired at frequency-1 and 453 ships' data at frequency-2. The matching results between the S25-RF2 and AIS data revealed that 880 ships were successfully matched (Figure 8). Specifically, 444 ships (94%) were matched at frequency-1, while 436 ships (96%) were matched at frequency-2. Across the distances of 2 km, 3 km, 6 km, 8 km, 13 km, and 18 km, the matching rates for frequency-1 S22-RF2 data were 41%, 22%, 16%, 7%, 4%, and 2%, respectively. The matching rates at the corresponding distance were 43%, 21%, 21%, 7%, 0.6%, and 0.2%, respectively, for frequency-2 S22-RF2 data. The overall matching rate for the S25-RF2 dataset was found to be 95%. Additionally, 6% of ships were found to be unmatched at frequency-1, compared to 4% at frequency-2.

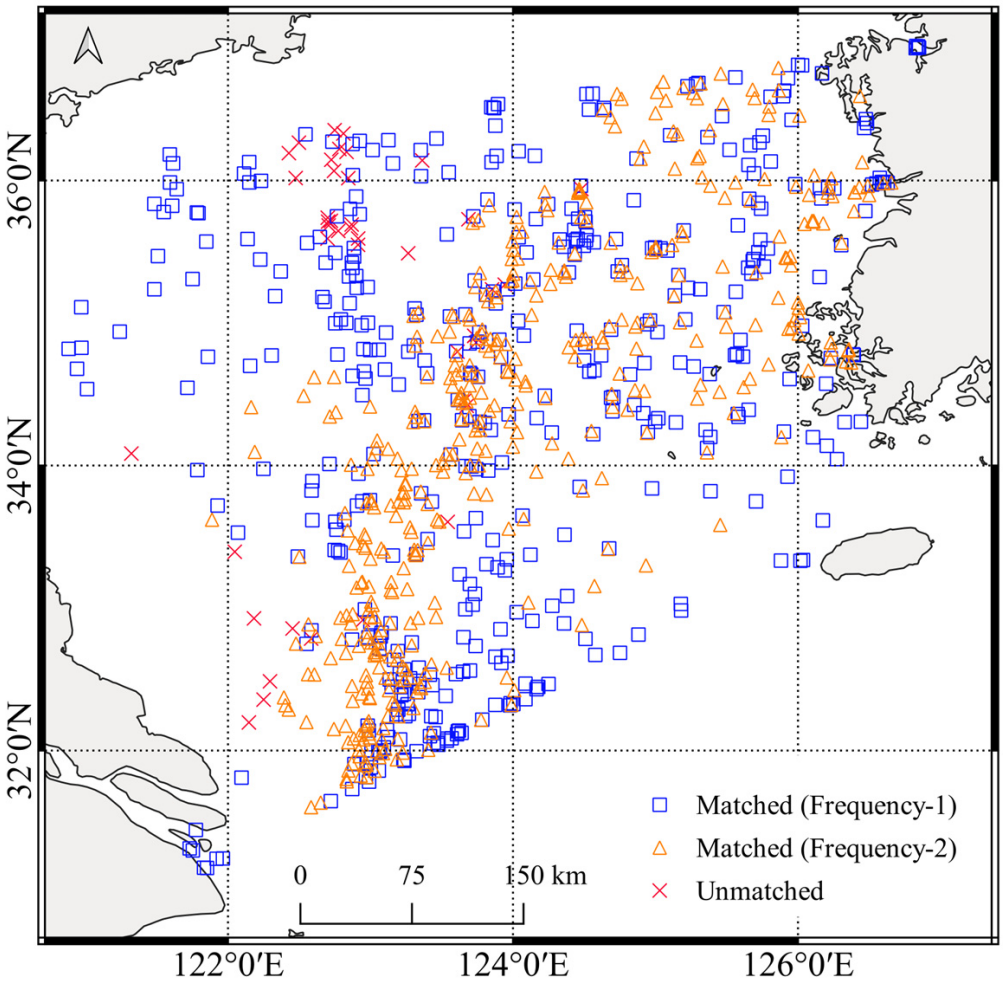


Figure 8. Ship identification results from different frequencies after matching the S25-RF2 dataset and AIS data on 25 September 2023. The blue rectangle indicates the position of a matched ship at frequency-1 (3.04~3.08 GHz), and the amber triangle represents the position of a matched ship at frequency-2 (9.37~9.41 GHz).

A total of 1088 ships' data records were found in the S25-RF3 dataset. Specifically, 694 ships' records were acquired at frequency-1, while 394 ships' records were obtained at frequency-2. The matching results depicted that a total of 1018 ships were identified (Figure 9). In addition, it was found that 644 ships were identified from the frequency-1 dataset of 694 ships, while 374 out of 394 ships' data were matched from frequency-2 data. The matching analysis between S25-RF3 and AIS data showed a matching rate of 92% at frequency-1 and 94% at frequency-2. The matching rates for frequency-1 S25-RF3 data across various distance thresholds were as follows: 31% at 2 km, 17% at 3 km, 17% at 6 km, 13% at 8 km, 4% at 13 km, and 2% at 18 km. For frequency-2 S25-RF3 data, the matching rates at the corresponding distances were 36%, 18%, 25%, 10%, 3%, and 1%, respectively. The total matching rate for the S25-RF3 dataset was found to be 93%. It was also found that 8% of ships were unmatched at frequency-1 and 6% at frequency-2.

Table 3 illustrates the key findings from the analysis of the RF dataset on 25 September 2023.

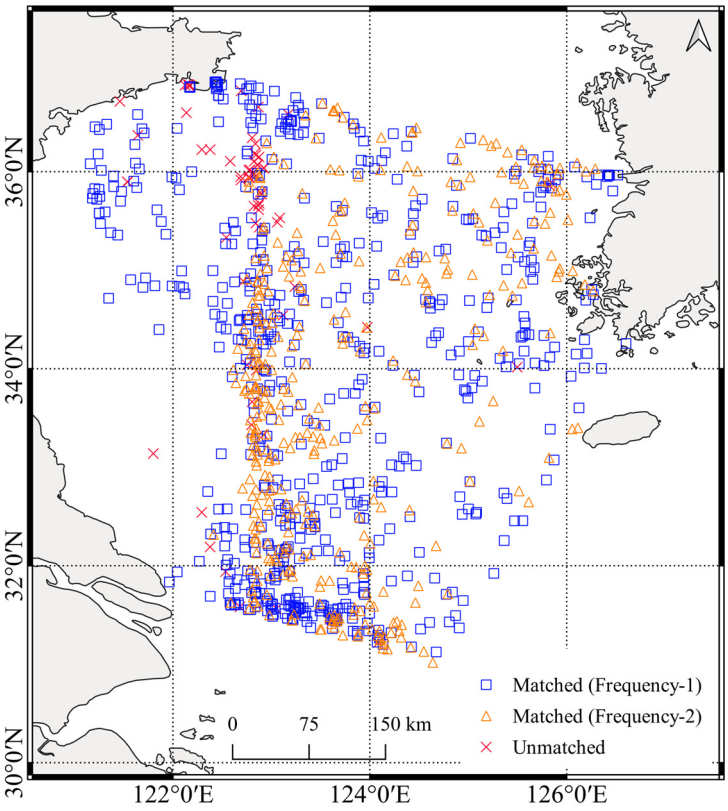


Figure 9. Ship identification results from different frequencies after matching the S25-RF3 dataset and AIS data on 25 September 2023. The blue rectangle indicates the position of a matched ship at frequency-1 (3.04~3.08 GHz), and the amber triangle represents the position of a matched ship at frequency-2 (9.37~9.41 GHz).

Table 3. Overview of the matching analysis for the RF dataset on 25 September 2023, detailing results for each specified distance across different frequencies.

Dataset (Frequency)	Total RF in Dataset	Total Matched Ship	Matched Ship (%)						Unmatched Ship (%)
			2 km	3 km	6 km	8 km	13 km	18 km	
S25-RF1 (Frequency-1)	429	376	42	13	20	7	2	1	13
S25-RF1 (Frequency-2)	537	484	42	16	20	7	2	1	10
S25-RF2 (Frequency-1)	469	444	41	22	16	7	4	2	6
S25-RF2 (Frequency-2)	453	436	43	21	21	7	0.6	0.2	4
S25-RF3 (Frequency-1)	694	644	31	17	23	13	4	2	8
S25-RF3 (Frequency-2)	394	374	36	18	25	10	3	1	6

3.3. Analysis of Matching Results from RF Dataset on 7 December 2023

The D07-RF1 dataset consisted of 1333 ship records, with 720 ships' data obtained at frequency-1 and 613 ships' data at frequency-2. The matching analysis between the D07-RF1 dataset and AIS data resulted in the successful identification of 1227 ships (Figure 10). Among these, 658 ships (91%) were matched at frequency-1, while 569 ships (92%) were matched at frequency-2. The matching rates for frequency-1 D07-RF data varied across different distance thresholds, with 18% at 2 km, 14% at 3 km, 26% at 6 km, 13% at 8 km, 14% at 13 km, and 6% at 18 km. For frequency-2 D07-RF1 data, the matching rates at the

corresponding distances were 21%, 10%, 24%, 13%, 14%, and 7%, respectively. The overall matching rate for the D07-RF1 dataset was calculated to be 92%. The analysis also revealed that 9% of ships were unmatched at frequency-1, with 8% unmatched at frequency-2.

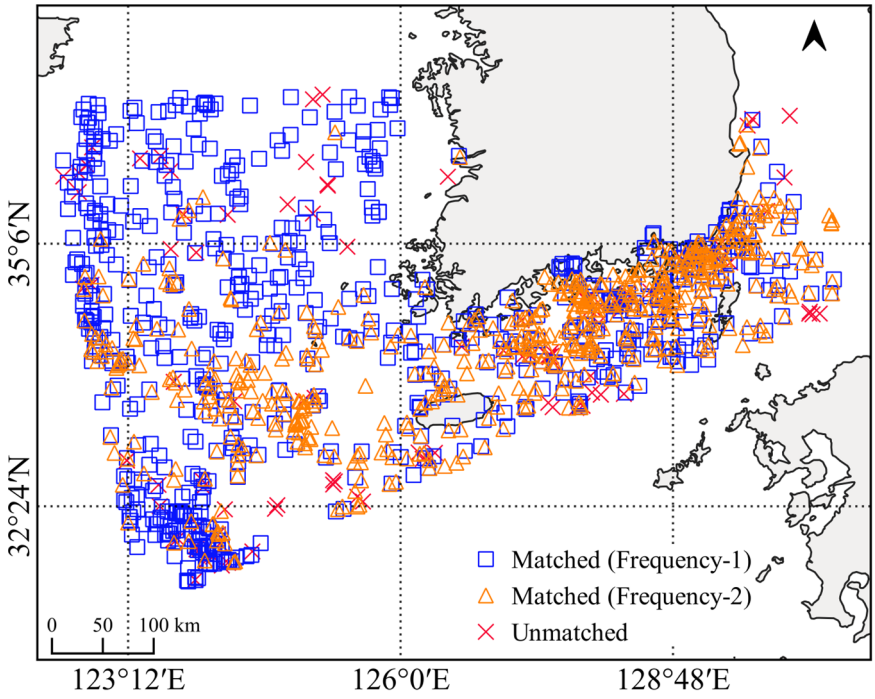


Figure 10. Ship identification results from different frequencies after matching the D07-RF1 dataset and AIS data on 7 December 2023. The blue rectangle indicates the position of a matched ship at frequency-1 (3.04~3.08 GHz), and the amber triangle represents the position of a matched ship at frequency-2 (9.37~9.41 GHz).

Table 4 highlights the overall outcomes of the analysis for the RF dataset on 7 December 2023.

Table 4. Overview of the matching analysis for the RF dataset on 7 December 2023, detailing results for each specified distance across different frequencies.

Dataset (Frequency)	Total RF in Dataset	Total Matched Ship	Matched Ship (%)						Unmatched Ship (%)
			2 km	3 km	6 km	8 km	13 km	18 km	
D07-RF1 (Frequency-1)	720	658	18	14	26	13	14	6	9
D07-RF1 (Frequency-2)	613	569	21	10	24	13	14	7	8

4. Discussion

For vessel monitoring, the AIS is a widely utilized system that significantly contributes to maritime safety by transmitting signals to provide positional information on ships and facilitate safe navigation. However, signal transmission might be interrupted due to intentional or unintentional causes, particularly when vessels attempt to operate undetected. In these cases, RF data can provide a reliable way to verify the AIS positions. This study evaluates the matching performance between RF and AIS data in the Yellow Sea and the western Korea Strait, according to the variations in frequency and distance. The RF datasets on 22 September, 25 September, and 7 December 2023 were separated based on the frequency range, denoted as frequency-1 (3.04~3.08 GHz) and frequency-2 (9.37~9.41 GHz). Afterward, a simple matching algorithm based on the distance was applied to each frequency

range for matching the RF and AIS position, and then the matching rate of RF-AIS was analyzed. The results depicted diverse matching accuracies across datasets and distance thresholds, reflecting differences in performance between frequency-1 and frequency-2. For the S22-RF1 dataset, frequency-1 achieved a peak matching rate of 54% at 2 km, and frequency-2 showed a slightly reduced rate of 46% while maintaining higher accuracy at longer distances (such as 1% at 18 km compared to 0.8%). In the S22-RF2 dataset, both frequency-1 and frequency-2 showed similar performance at shorter distances. However, frequency-2 exceeded frequency-1 at longer distances, exhibiting a more gradual decline in matching accuracy. The S25-RF1 dataset revealed the slightest differences between frequencies, with both achieving similar matching rates at short and long distances (such as 42% at 2 km and 1% at 18 km). In contrast, for S25-RF3, frequency-2 consistently exceeded frequency-1 at distances greater than 6 km, achieving 25% compared to 17% at 6 km and 10% compared to 13% at 8 km. Similarly, the D07-RF1 dataset showed a consistent trend where frequency-2 exceeded frequency-1 across all distances, especially at shorter distances (such as 21% at 2 km compared to 18%). Overall, frequency-2 exhibited more stable and robust performance across most datasets, particularly at longer distances. Moreover, the analysis results also showed that the overall matching rate of the S22-RF1, S22-RF2, S22-RF3, S25-RF1, S25-RF2, S25-RF3, and D07-RF1 datasets were 92%, 97%, 97%, 88%, 95%, 93%, and 92%, respectively. Specifically, in the S22-RF1 dataset, the average matching rates for both frequencies were 50% at 2 km, 14% at 3 km, 18% at 6 km, 12% at 8 km, 2% at 13 km, and 1% at 18 km. In addition, in the S22-RF2 dataset, the average matching rates were 45%, 19%, 20%, 9%, 1%, and 0.5% for the respective distances. For the S22-RF3 dataset, the average matching rates at 2 km, 3 km, 6 km, 8 km, 13 km, and 18 km were 46%, 17%, 23%, 6%, 2%, and 0.9%, respectively. Furthermore, in the S25-RF1 dataset, both frequencies showed average matching rates of 42% at 2 km, 14% at 3 km, 20% at 6 km, 7% at 8 km, 2% at 13 km, and 1% at 18 km. For the S25-RF2 dataset, the average matching rates corresponding to these distances were 42%, 21%, 19%, 7%, 2%, and 1%. Similarly, in the S25-RF3 dataset, the average matching rates calculated were 33% at 2 km, 17% at 3 km, 24% at 6 km, 11% at 8 km, 3% at 13 km, and 1% at 18 km. Finally, in the D07-RF1 dataset, the calculated average matching rates at both frequencies were 20% for 2 km, 12% for 3 km, 25% for 6 km, 13% for 8 km, 14% for 13 km, and 6% for 18 km. According to the analysis, the average matching rates consistently decrease as the distance increases across both frequencies. Shorter distances, such as 2 km, demonstrate significantly higher matching rates, indicating signal stability at closer ranges. However, as the distance extends to intermediate and long ranges (e.g., 8 km and beyond), the matching rates drop sharply, reflecting the impact of signal attenuation.

5. Conclusions

This study evaluated the matching performance between RF and AIS data based on the frequency across various datasets in the Yellow Sea and the western Korea Strait. The average matching rates across all datasets were 92% for S22-RF1, 97% for S22-RF2, 97% for S22-RF3, 88% for S25-RF1, 95% for S25-RF2, 93% for S25-RF3, and 92% for D07-RF1. The analysis revealed that frequency-2 (9.37~9.41 GHz) generally outperformed frequency-1 (3.04~3.08 GHz), particularly at longer distances, with a more stable decline in matching accuracy. On the other hand, frequency-1 showed stronger matching performance at shorter distances. Based on the analysis, it can be assumed that frequency-2 might be more effective for long-range vessel monitoring due to its relatively stable performance at greater distances, while frequency-1 could be more suitable for short-range applications, given its higher accuracy at closer ranges.

Author Contributions: Conceptualization, C.-S.Y. and S.J.K.C.; methodology, C.-S.Y. and S.J.K.C.; software, S.J.K.C.; validation, C.-S.Y. and S.J.K.C.; formal analysis, C.-S.Y. and S.J.K.C.; investigation, C.-S.Y. and S.J.K.C.; resources, C.-S.Y. and S.J.K.C.; data curation, C.-S.Y. and S.J.K.C.; writing—original draft preparation, S.J.K.C.; writing—review and editing, C.-S.Y. and S.J.K.C.; visualization, C.-S.Y. and S.J.K.C.; supervision, C.-S.Y.; project administration, C.-S.Y.; funding acquisition, C.-S.Y. All authors have read and agreed to the published version of the manuscript.

Funding: This research was financially supported under the "Development of Maritime Domain Awareness Technology for Sea Power Enhancement (PEA0332)" project funded by the Korea Institute of Ocean Science & Technology, and the Ministry of Foreign Affairs (IUU Project), Republic of Korea.

Data Availability Statement: Data are contained within the article.

Conflicts of Interest: The authors declare no conflicts of interest.

References

1. Sheng, P.; Yin, J. Extracting shipping route patterns by trajectory clustering model based on Automatic Identification System data. *Sustainability* **2018**, *10*, 2327. [CrossRef]
2. Rong, H.; Teixeira, A.P.; Soares, C.G. Ship trajectory uncertainty prediction based on a gaussian process model. *Ocean Eng.* **2019**, *182*, 499–511. [CrossRef]
3. Yan, Z.; Song, X.; Zhong, H.; Yang, L.; Wang, Y. Ship classification and anomaly detection based on spaceborne AIS data considering behavior characteristics. *Sensors* **2022**, *22*, 7713. [CrossRef] [PubMed]
4. International Maritime Organization. Adoption of New and Amended Performance Standards. 1998. Available online: https://wwwcdn.imo.org/localresources/en/OurWork/Safety/Documents/AIS/Resolution%20MSC.74(69).pdf (accessed on 11 December 2024).
5. International Maritime Organization. *Strategic Plan for the Organization (for Six-Year Period 2012 to 2017)*; Resolution A 1037(27); International Maritime Organization: London, UK, 2011; pp. 3–4.
6. Harati-Mokhtari, A.; Wall, A.; Brookes, P.; Wang, J. Automatic identification system (AIS): A human factors approach. *J. Navig.* **2007**, *60*, 373–389. [CrossRef]
7. Chen, X.; Liu, Y.; Achutan, K.; Zhang, X. A ship movement classification based on Automatic Identification System (AIS) data using convolution neural network. *Ocean Eng.* **2020**, *218*, 108182. [CrossRef]
8. Hong, D.-B.; Yang, C.-S.; Kim, T.-H. Investigation of passing ships in inaccessible areas using satellite-based Automatic Identification System (S-AIS) data. *Korean J. Remote Sens.* **2018**, *34*, 579–590.
9. Metcalfe, K.; Bréheret, N.; Chauvet, E.; Collins, T.; Curran, B.K.; Parnell, R.J.; Turner, R.A.; Witt, M.J.; Godley, B.J. Using satellite AIS to improve our understanding of shipping and fill gaps in ocean observation data to support marine spatial planning. *J. Appl. Ecol.* **2018**, *55*, 1834–1845. [CrossRef]
10. Fournier, M.; Casey Hilliard, R.; Rezaee, S.; Pelot, R. Past, present, and future of the satellite-based automatic identification system: Areas of applications (2004–2016). *WMU J. Marit. Aff.* **2018**, *17*, 311–345. [CrossRef]
11. Venskus, J.; Treigys, P.; Bernatavičienė, J.; Tamulevičius, G.; Medvedev, V. Real-Time Maritime Traffic Anomaly Detection Based on Sensors and History Data Embedding. *Sensors* **2019**, *19*, 3782. [CrossRef]
12. Wang, C.M.; Li, Y.; Min, L.; Chen, J.; Lin, Z.; Su, S.; Zhang, Y.; Chen, Q.; Chen, Y.; Duan, X.; et al. Intelligent marine area supervision based on AIS and radar fusion. *Ocean Eng.* **2023**, *285*, 115373.
13. Zhao, L.; Fu, X. A novel index for real-time ship collision risk assessment based on velocity obstacle considering dimension data from AIS. *Ocean Eng.* **2021**, *240*, 109913. [CrossRef]
14. Shin, D.-W.; Yang, C.-S. Classification of ship type from combination of HMM–DNN–CNN models based on ship trajectory features. *Remote Sens.* **2024**, *16*, 4245. [CrossRef]
15. Graziano, M.D.; Renga, A.; Moccia, A. Integration of Automatic Identification System (AIS) data and single-channel Synthetic Aperture Radar (SAR) images by SAR-based ship velocity estimation for maritime situational awareness. *Remote Sens.* **2019**, *11*, 2196. [CrossRef]
16. Shin, D.-W.; Yang, C.-S.; Chowdhury, S.J.K. Enhancement of small ship detection using polarimetric combination from Sentinel−1 imagery. *Remote Sens.* **2024**, *16*, 1198. [CrossRef]
17. Kang, M.; Ji, K.; Leng, X.; Lin, Z. Contextual region-based convolutional neural network with multilayer fusion for SAR ship detection. *Remote Sens.* **2017**, *9*, 860. [CrossRef]
18. Chang, Y.-L.; Anagaw, A.; Chang, L.; Wang, Y.C.; Hsiao, C.-Y.; Lee, W.-H. Ship detection based on YOLOv2 for SAR imagery. *Remote Sens.* **2019**, *11*, 786. [CrossRef]

19. Louart, M.; Szkolnik, J.-J.; Boudraa, A.-O.; Le Lann, J.-C.; Roy, F.L. Detection of AIS messages falsifications and spoofing by checking messages compliance with TDMA protocol. *Digit. Signal Process.* **2023**, *136*, 103983. [CrossRef]
20. Dark Shipping Solutions, 2024. Dark Vessel Detection with Satellite-Based RF Tracking. Available online: https://www.darkshipping.com/solutionsexpanded/dark-vessel-detection-with-satellite-based-rf-tracking (accessed on 11 December 2024).
21. Travis Turgeon, 2023. Radio Frequency Collection: Securing the Maritime Domain. Available online: https://www.darkshipping.com/post/securing-the-maritime-domain-with-rf-data (accessed on 10 December 2024).
22. SatMagazine, 2023. Focus: Unseenlabs, A European Leader in RF Signals Detection from Space for Maritime Surveillance. Available online: http://satmagazine.com/story.php?number=327566464 (accessed on 10 December 2024).
23. Yang, C.-S.; Cho, J. Matching method for ship identification using satellite-based radio frequency sensing data. *Korean J. Remote Sens.* **2024**, *40*, 219–228.
24. Marine Radar Onboard Ships: An Overview. Available online: https://seamankowts.net/marine-radar-onboard-ships-an-overview/ (accessed on 10 January 2024).

Disclaimer/Publisher's Note: The statements, opinions and data contained in all publications are solely those of the individual author(s) and contributor(s) and not of MDPI and/or the editor(s). MDPI and/or the editor(s) disclaim responsibility for any injury to people or property resulting from any ideas, methods, instructions or products referred to in the content.